Photolytic degradation of commonly used pesticides adsorbed on silica particles

Boulos Samia, Joanna Socorro, Amandine Durand, Etienne Quivet, Henri Wortham

Science of the Total Environment 949 (2024) 174964

Contents lists available at ScienceDirect

Science of the Total Environment

journal homepage: www.elsevier.com/locate/scitotenv

Photolytic degradation of commonly used pesticides adsorbed on silica particles

Boulos Samia *, Joanna Socorro, Amandine Durand, Etienne Quivet, Henri Wortham

Aix Marseille Univ, CNRS, LCE, Marseille, France

HIGHLIGHTS

- Investigation of the heterogeneous atmospheric photolysis of pesticides.
- Fipronil shows the highest reactivity to both xenon lamp and sunlight.
- Pesticide mixture can influence differently the photolysis constant rates.
- Pesticides in a mixture can act as a photosensitizer.
- Complexity to transfer laboratory photolysis rate constants to the real atmosphere.

GRAPHICAL ABSTRACT

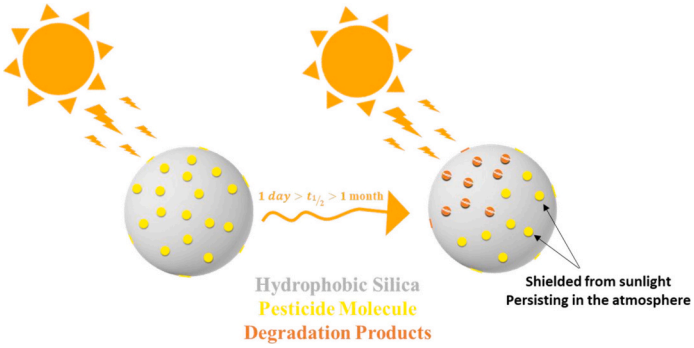

ARTICLE INFO

Editor: Damia Barcelo

Keywords:
Atmospheric reactivity
Phytopharmaceutical products
Photolysis
Heterogeneous reactivity
Kinetics
Aerosols

ABSTRACT

The currently used pesticides are mostly semi-volatile organic compounds. As a result, a fraction of them can be adsorbed on atmospheric aerosol surface. Their atmospheric photolysis is poorly documented, and gaps persist in understanding their reactivity in the particle phase. Laboratory experiments were conducted to determine the photolysis rates of eight commonly used pesticides (i.e., cyprodinil, deltamethrin, difenoconazole, fipronil, oxadiazon, pendimethalin, permethrin, and tetraconazole) using a flow reactor. These pesticides were individually adsorbed on hydrophobic silica particles and exposed to a filtered xenon lamp to mimic atmospheric aerosols and sunlight irradiation, respectively.

The estimated photolysis rate constants ranged from less than $(3.4 \pm 0.3) \times 10^{-7}$ s^{-1} (permethrin; >47.2 days) to $(3.8 \pm 0.2) \times 10^{-5}$ s^{-1} (Fipronil; 0.4 days), depending on the considered compound. Moreover, this study assessed the influence of pesticide mixtures on their photolysis rates, revealing that certain pesticides can act as photosensitizers, thereby enhancing the reactivity of permethrin and tetraconazole. This study underscores the importance of considering photolysis degradation when evaluating pesticide fate and reactivity, as it can be a predominant degradation pathway for some pesticides. This contributes to an enhanced understanding of their behavior in the atmosphere and their impact on air quality.

* Corresponding author.
E-mail address: boulos.samia@univ-amu.fr (B. Samia).

https://doi.org/10.1016/j.scitotenv.2024.174964
Received 24 May 2024; Received in revised form 19 July 2024; Accepted 20 July 2024
Available online 25 July 2024

1. Introduction

The excessive use of pesticides has alarmed the scientific community due to their detrimental effects on human health, such as accelerating Parkinson's disease (Li et al., 2024; Paul et al., 2022), inducing prostate cancer (Pardo et al., 2020), and affecting respiratory functions (Ye et al., 2017). It also impacts the environment by contaminating all its components (air, water, soil and biota), resulting in the death of numerous living organisms (Pisa et al., 2021). Each year, pesticide pollution leads to a minimum of nine million premature deaths worldwide (HEAL, 2023).

In agriculture, several pesticide application methods lead to their dispersion into the air, such as aerial spraying that uses airplanes or drones to treat large agricultural areas (Gupte et al., 2012; Natu and Kulkarni, 2016) and ground spraying that uses tractors (Abbott et al., 1987). These two techniques generate tiny droplets that wind carries into the atmosphere. Furthermore, volatilization (Zivan et al., 2016) and wind erosion (Glotfelty et al., 1989), can also contribute to carrying these chemicals into the air. Moreover, Pimentel and Levitan (1986) mentioned that due to spray drift, <1 % of pesticides reach their intended targets, resulting in over 99 % of the chemicals being transferred to non-targeted parts of ecosystems, including the atmosphere.

Once released into the atmosphere, pesticides distribute among the aqueous, gaseous, and particulate phases based on their physical and chemical properties. However, their presence in the aqueous phase is generally limited due to their low water solubility and the small fraction (10 to 15 %) of the troposphere occupied by clouds. Currently, many pesticides in use are semi-volatile compounds, and a fraction of them is adsorbed onto the surface of atmospheric particles (Sauret et al., 2008). On these surfaces, they may undergo direct and indirect photochemical degradation, potentially leading to the formation of secondary products that could be more toxic than their parents.

Despite the presence of these pesticides in the particulate phase, and because the first pesticides used, such as organochlorines, were present exclusively in the gaseous phase of the atmosphere, the majority of studies on pesticide reactivity have focused on the gaseous phase fraction, considering their photolysis (Muñoz et al., 2014 and references therein) and their interactions with the three main atmospheric oxidants: ozone (O_3) (Borrás et al., 2017), hydroxyl radicals (OH) (Le Person et al., 2007; Vera et al., 2015; Zhou et al., 2011, 2010), and nitrate radicals (NO_3) (Aschmann et al., 2005a, 2005b; Aschmann and Atkinson, 2006; Cheng et al., 2017).

In addition, to date, for the approval and market entry of pesticides, concerning their atmospheric behavior, regulatory agencies rely exclusively on their homogeneous reactivity with ·OH radicals, using data estimated solely by the AOPWIN™ model (Atmospheric Oxidation Program for Microsoft Windows, Software, Meylan and Howard, 1993). This omission of the particulate phase reactivity leads to an underestimation of their persistence in the atmosphere, as demonstrated by the few recent studies on the heterogeneous degradation of pesticides by atmospheric oxidants (Mattei et al., 2019a, 2019b, 2019c; Socorro et al., 2015, 2016a, 2016b). These studies show that the reactivity of pesticides is approximately 100 times slower when they are present in the particulate phase compared to the gaseous phase, resulting in prolonged atmospheric persistence and potential for long-distance transport.

Nonetheless, there has been a lack of research on the interaction between sunlight irradiation and pesticides adsorbed on atmospheric particles. To our knowledge, only two studies have examined the photolysis of pesticides on solid phases. Bossan et al. (1995) exposed eight pesticides adsorbed on three types of surfaces: kaolinite, fly ash, and ammonium sulfate, using a lamp with a spectrum ranging from 260 to 700 nm. Aregahegn et al. (2018) investigated the photolysis of solid films of neonicotinoids using two lamps: a low-pressure mercury lamp emitting at 254 nm and a low-pressure organic phosphor-coated mercury lamp emitting at 313 nm. Many other studies focus on the photodegradation of pesticides adsorbed on solid supports such as seed or leaf surfaces. However, since the nature of the surface can influence photolysis kinetics, these studies cannot be considered for atmospheric photo-reactivity assessments.

These two studies focusing on atmospheric particle surface are insufficient to address the significant gaps and uncertainties in calculating the atmospheric half-lives of particulate pesticides exposed to sunlight. Therefore, this study aims to determine the photolysis rates of eight pesticides (Cyprodinil, deltamethrin, difenoconazole, fipronil, oxadiazon, pendimethalin, permethrin, and tetraconazole) representative of various chemical classes. They were selected based on their partition between gas and particulate phases, toxicity, and persistence in the atmosphere (Désert et al., 2018). These pesticides were adsorbed on hydrophobic silica particles mimicking atmospheric particles crustal in origin and exposed to a xenon lamp. The laboratory results were used to carry out an extrapolation of the findings to real sunlight conditions. Finally, since multiple pesticides are often adsorbed on the same atmospheric particles, this study provides insights on the influence of pesticide mixture on the photolysis rate constant of the eight pesticides under investigation.

2. Materials and methods

2.1. Chemicals

Cyprodinil (purity 99.8 %), deltamethrin (99.7 %), difenoconazole (97.0 %), fipronil (97.5 %), oxadiazon (99.9 %), pendimethalin (98.8 %), permethrin (98.3 %), and tetraconazole (99.0 %) were purchased from Sigma-Aldrich (PESTANAL®, analytical standard) and used as received. The chemical structures of the eight pesticides under study are presented in Fig. SI1 and their physicochemical properties are provided in Table SI1.

2.2. Particles coating

Hydrophobic silica particles (AEROSIL R812, Degussa) were selected to mimic atmospheric mineral aerosols. This choice is based on the observation that 20 to 30 % of inorganic particles in the actual atmosphere are believed to be oxides containing SiO_2 (Seinfeld and Pandis, 2016). These particles were characterized by a SiO_2 purity $\geq$ 99.8 %, an average primary particle size of 7 nm, and a specific surface area of (260 $\pm$ 30) $m^2 \cdot g^{-1}$ (based on Brunauer-Emmett-Teller (BET) analysis conducted at boiling temperature of N_2, 77 K).

The SiO_2 particles were coated with the eight pesticides, either individually or in combination, using the solid/liquid adsorption method that has been reported previously (Samia et al., 2024 and reference therein). To prevent any potential photodegradation of pesticides, the particle coating process was conducted in the dark. This involved mixing 5 mL of pesticide solution at 20 $mg \cdot L^{-1}$ in dichloromethane (HPLC grade $\geq$ 99.8 % purity, Sigma-Aldrich) with 500 mg of silica particles and around 150 mL of dichloromethane in a 500 cm^3 Pyrex flask. After 15 min of ultrasonication, dichloromethane was evaporated for about 30 min using a rotary evaporator (Rotavapor R-114, Büchi Switzerland) at 40 °C (Water bath B-480, Büchi Switzerland) and 850 $\pm$ 85 mbar (Vac® V500 Vacuum controller B-721, Büchi Switzerland).

The efficacy of the particle coating process was validated by measuring the initial concentration of the pesticides immediately after coating the silica particles with the pesticide and before placing them in the reactor to be exposed to artificial light. For this purpose, a fraction of the particles was extracted and analyzed to determine the initial concentrations of the studied pesticides. This step ensured the consistency and robustness of the coating process by calculating the coverage rate of particles by pesticides after each coating. The loading rate of silica particles by pesticides was about 0.02 %, while the percentage of the total coated particle surface was 2.8 %, which is significantly less than a monolayer and prevents any shielding effect (Mattei et al., 2019a), with

the assumption of uniform particle surface coverage and spherical particle geometry (calculation details in SI).

2.3. Photolysis experimental setup

To study pesticide photolysis, we adopted and adapted the experimental setup previously used for investigating the heterogeneous reactivity of pesticides with atmospheric oxidants (Mattei et al., 2019a; Samia et al., 2024).

About 500 mg of coated silica particles were placed into a 500 cm^3 Pyrex bulb attached to a modified rotary evaporator (Laborota 4000 efficient, Heidolph) and maintained at a constant temperature of 25 ± 1 °C using a water bath (Cf. Fig. 1). The constant rotation of the bulb ensured uniform particle exposure to the 300 W xenon lamp (LOT, Oriel), positioned 10 cm above the reactor surface, to simulate sunlight irradiation.

A continuous flow of purified and dried air was generated at 500 $mL{\cdot}min^{-1}$ using a Zero air generator ZA 1500P (F-DGS), ensuring complete air volume renewal in the reactor every minute. This continuous renewal dilutes and removes any potential secondary oxidants formed by the photolysis of pesticides, maintaining their concentrations at extremely low levels and preventing significant further reactions with the pesticides. Socorro et al. (2016b), using a similar experimental setup to investigate pesticide reactivity with OH radicals and ozone, demonstrated that identified degradation products exclusively resulted from their reactivity with these two oxidants without the involvement of secondary products or radicals. This allows for confidently disregarding the reactivity of pesticides with potential secondary oxidants in favor of their degradation induced by light.

Additionally, this flow was sufficiently moderate to avoid particle loss by entrainment towards the outside of the reactor. This airflow is divided into two paths prior to entering the reactor (Cf. Fig. 1). The first 250 $mL{\cdot}min^{-1}$ stream passed through an ultra-pure water-filled bubbler, producing air fully saturated with 100 % humidity while the dry second stream at 250 $mL{\cdot}min^{-1}$ diluted the first one, achieving a consistent relative humidity (RH) of 55 ± 5 % in the reactor.

The humidity level was measured using a hygrometric probe (Hydrolog NT, Rotronic, USA), which also allows simultaneous monitoring of the temperature inside the reactor. The exposure to xenon lamp light lasted for 26 h to accommodate the relatively slow degradation of pesticides and to maximize the number of data points collected.

2.4. Exposure to xenon lamp

To measure the spectral irradiance received by the adsorbed pesticides in the reactor during kinetic experiments, a spectroradiometer (SR-501, Spectral Evolution) was placed at different positions inside the Pyrex bulb of the rotary reactor, to measure the lamp's average emission spectrum (Cf. Fig. SI2).

For comparison purposes, a reference solar spectrum based on the American Society for Testing and Materials (ASTM) G 173-03 standard from SMARTS v.2.9.2 (AM1.5 Direct) was used. This standard spectrum is obtained under clear skies, at an inclination of 37° with respect to the equator (elevation of 41.8° above the horizon), averaged over a year across the 48 contiguous states of the United States of America (Gueymard et al., 2002).

Xenon lamps emit a continuous spectrum of light similar to natural sunlight but with higher intensity, especially in the UV range, and at lower wavelengths (down to about 200 nm for the xenon lamp compared to 295 nm for sunlight).

The increased intensity between the two light sources is beneficial as it only corresponds to an increase in actinic flux (photon.s^{-1}.$surface^{-1}$), enhancing degradation kinetics, and reducing the duration of experiments. The degradation kinetics are linearly dependent on the actinic flux, allowing to extrapolate the results obtained with the xenon lamp to solar light using a simple proportionality rule.

The wavelength difference between the two light sources is much more problematic because the photolysis of a given molecule is highly dependent on the wavelength it receives. Fortunately, the Pyrex wall of the reactor filters out UV radiation and cuts off light at 280 nm. After filtration by the Pyrex, the gap between the solar light and the lamp light is only about 15 nm (280 for the lamp compared to 295 for the sun). Even though the difference between the two spectra is only 15 nm, it remains a challenge because some molecules can absorb light and undergo photolysis between 280 nm and 295 nm but will no longer react, or will react more slowly, beyond 295 nm. Thus, xenon lamps enable more efficient photochemical processes compared to natural sunlight.

To eliminate all uncertainties regarding the results due to the difference between solar light and xenon lamp, a study in 2020 compared the atmospheric reactivity of iodine molecules adsorbed on silica particles using the same experimental setup for both the filtered-xenon lamp and real sunlight exposure, with the setup placed outdoors. Iodine molecules absorb between 280 and 600 nm. They concluded that the photolysis constants obtained in both cases were of the same order of magnitude, thus resolving the issue of this difference (Figueiredo et al., 2020).

Furthermore, to reduce disparities, a corrective factor F_{light} was calculated to provide an initial estimation of the photolysis frequency J' when exposed to sunlight (Eq. (1)). This factor corresponds to the ratio between the integration of the area under the lamp's emission spectrum curve and the integration of the area under the measured average solar emission spectrum curve, at the same wavelengths. An F_{light} was calculated for each pesticide's absorption wavelength range. Calculating J' helps estimate the atmospheric half-life for each pesticide under sun

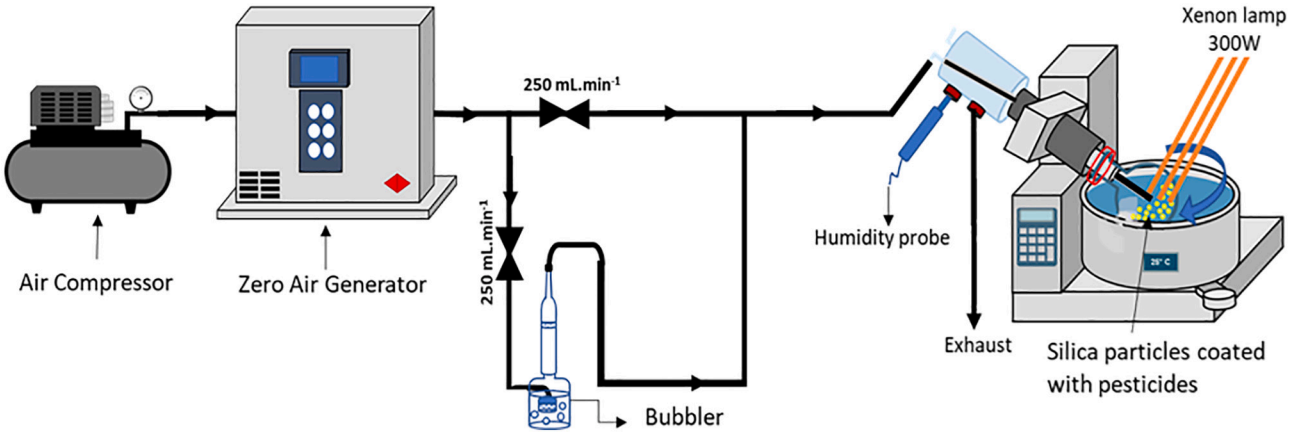

Fig. 1. Experimental setup used to study the heterogeneous photolysis of pesticides adsorbed on silica particles.

exposure, aiming to mimic real atmospheric conditions.

$$J' = \frac{J}{F_{light}} \quad (1)$$

Moreover, UV–visible spectra were obtained for each pesticide at various concentrations on the surfaces of silica particles, employing a spectrophotometer (Jasco V-670 spectrophotometer, horizontal integrating sphere PIN-757), capable of conducting solid-phase measurements. The particles and their preparation match those used in experiments, ensuring a representative spectrum for each pesticide under experimental conditions. Detailed UV–visible spectra for each pesticide, along with the spectrophotometer's specifications, are provided in SI.

Please note that in the following sections, we will always be referring to the filtered xenon lamp.

2.5. Pesticide extraction and analysis

Pesticides adsorbed on silica particles were extracted by accelerated solvent extraction (ASE 300, Dionex). Each sample of 40 mg of particles was placed in a 33 mL stainless steel extraction cell and spiked with an internal standard solution of TPP (Triphenyl phosphate, 99.9 %, Sigma-Aldrich) and then extracted with dichloromethane at 100 °C, 100 bars. Following extraction, analytes dissolved in dichloromethane were concentrated under a nitrogen flow using a concentration workstation (TurboVap II, Biotage) until a 500 μL extract was obtained. Further information regarding the ASE extraction and concentration step can be found in Socorro et al. (2015).

These solutions underwent analysis using gas chromatography coupled to tandem mass spectrometry (GC–MS/MS), employing a Trace GC Ultra (Thermo Scientific) coupled to a TSQ Quantum™ Triple Quadrupole (Thermo Scientific) with electron impact ionization (70 eV). The parameters and experimental conditions of the GC–MS/MS analysis, along with a chromatogram of the 8 pesticides and the internal standard, are presented in the SI.

2.6. Determination of photolysis rate constants and atmospheric half-lives

The photolysis reaction of pesticides adsorbed on silica particles, induced by xenon lamp radiation is a first-order dissociation reaction (Finlayson-Pitts and Pitts, 2000) that has a kinetic constant J (s^{-1}), referred to as the photolysis rate constant.

The photolysis rate constant over all wavelengths of radiation is defined by Eq. (2):

$$J = \int \sigma_{(\lambda)} \times \int \phi_{(\lambda)} \times \int F_{(\lambda)} \quad (2)$$

where $\sigma_{(\lambda)}$ is the absorption cross-section, which describes the efficiency of a molecule in absorbing light at a specific wavelength ($cm^2 \cdot molecule^{-1}$), $\phi_{(\lambda)}$ is the quantum yield, representing the probability of photolysis occurring when a molecule absorbs a photon of light and is defined as the ratio of the number of transformed molecules to the number of absorbed photons ($molecule \cdot photon^{-1}$), and $F_{(\lambda)}$ is the actinic solar flux, which describes the intensity of available radiation that can be absorbed by the pesticide, typically measured in photons ($photon \cdot cm^{-2} \cdot s^{-1}$).

In the present, determining these parameters or finding them in existing literature for the pesticides under study presents challenges. Therefore, we opted to calculate the J constant by monitoring the evolution of pesticides concentrations over the 26 h.

However, the decrease in pesticide concentration on silica surfaces involves various processes, including photolysis, hydrolysis, and desorption, as shown in Eq. (3).

$$-\frac{d[Pesticide_{ads}]}{dt} = k_{obs} \times [Pesticide_{ads}] = J \times [Pesticide_{ads}] + k_{desorption} \times [Pesticide_{ads}] + k_{hydrolysis} \times [Pesticide_{ads}] \quad (3)$$

In this equation, k_{obs} (s^{-1}) is the observed first-order rate constant, J (s^{-1}) is the photolysis rate constant, $k_{desorption}$ (s^{-1}) is the desorption first-order rate constant, $k_{hydrolysis}$ (s^{-1}) is the hydrolysis rate constant, t (s) is the time of exposure to xenon lamp radiation and [Pesticide $_{ads}$] is the normalized pesticide concentration adsorbed on the silica particles.

In order to determine the photolysis rate constant J, a light-free control experiment was conducted under the same experimental conditions, prior to each pesticide photolysis experiment. The decays of normalized concentrations relative to their initial concentration of the 8 pesticides under study caused by hydrolysis and desorption are presented in Fig. SI3.

This was carried out to quantify the potential loss of pesticides due to hydrolysis or desorption over the 26 h of experiment. As a result, considering the uncertainties in our experiments, minimal to zero losses were observed for all 8 pesticides under study. The highest loss rate of $(6.7 \pm 5.3) \times 10^{-7}$ s^{-1}, was obtained for pendimethalin.

To determine the degradation kinetics, for each pesticide, any non-zero loss rates was subtracted in advance from the raw data.

Furthermore, by integrating Eq. (3) and subtracting the rate constants associated with desorption and hydrolysis, the J photolysis rate constant is determined via linear regression of the following Eq. (4):

$$ln\left(\frac{[Pesticide_{ads}]_t}{[Pesticide_{ads}]_0}\right) = -J \times t \quad (4)$$

Additionally, pesticide atmospheric half-lives ($t_{1/2}$ in s) towards direct photolysis by the xenon lamp are obtained by using Eq. (5):

$$t_{1/2} = \frac{ln2}{J} \quad (5)$$

The obtained half-lives are then converted into days, considering 12-hour exposure to light per day. These calculations correspond to the direct photolysis of studied pesticides with respect to the lamp used. To better simulate actual atmospheric conditions, all of these calculations will be adjusted using the F_{light} factor.

3. Results and discussion

3.1. Solar spectral irradiance and pesticides absorption

For a precise interpretation of the kinetic results and their extrapolation to real environmental conditions, it is crucial to accurately characterize the actinic flux of the employed lamp and compare it to solar radiation. The same spectroradiometer was used for both the lamp and the sun. Solar spectrum data was collected on July 20, 2015, in Marseille, France, (Latitude: N 43°18′21.3″ and Longitude: E 5°22′46.4″), from 9 am to 1 pm, at regular one-hour intervals to obtain an average spectrum (Data collected is presented in SI).

The ASTM G173-03 solar reference standard was used to compare these actinic flux measurements. The measured solar spectra at 12 pm in Marseille closely match the reference, validating the spectroradiometer's accuracy. The average solar spectral irradiance is then calculated for

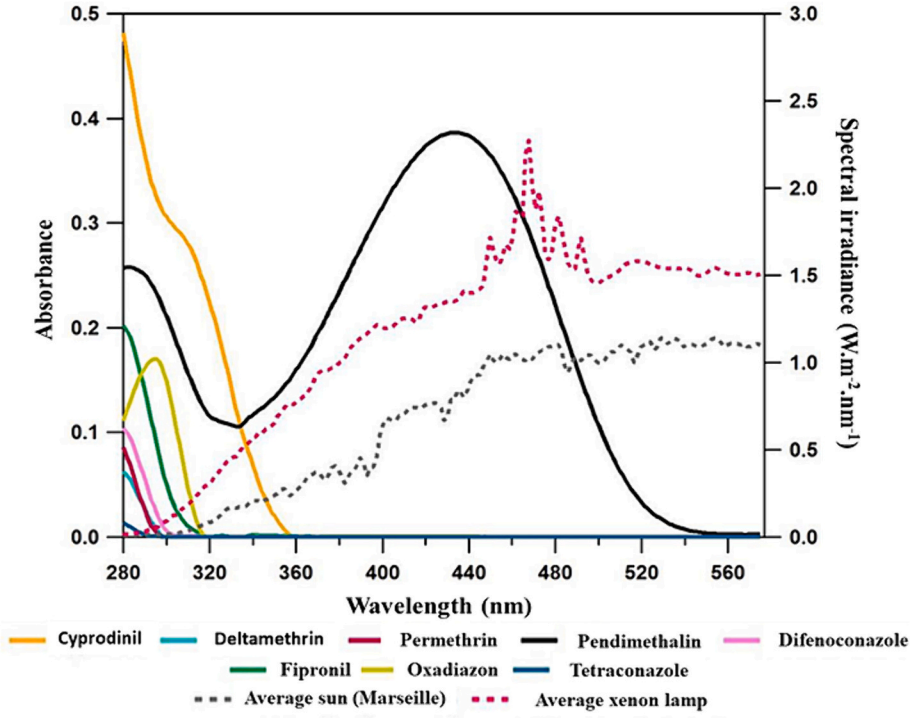

Fig. 2. Average spectral irradiance measured from the xenon lamp and the sun (in Marseille), along with the absorbances of the 8 pesticides adsorbed on silica particles.

comparison with the lamp's irradiance.

A comparison between the average lamp emission spectrum and the average sun spectrum in Marseille, along with the absorption spectra of the 8 pesticides adsorbed on silica particles at concentrations of 2 $mg{\cdot}g^{-1}$, is presented in Fig. 2.

As previously mentioned, these results indicate that the irradiance received by the pesticides inside the reactor is approximately 1.5 times more intense than solar irradiance. Furthermore, below 295 nm, the sun emits negligible radiation, while the filtered xenon lamp continues emitting radiation down to 280 nm. Thus, the xenon lamp emits more intense radiation than the sun and across a broader UV emission range, thereby more effectively photolyzing pesticides that absorb radiation from 295 nm down to 280 nm.

As we can see, seven pesticides exhibit an absorption band between 280 and 360 nm. Pendimethalin is unique, possessing two consecutive absorption bands with maxima around 280 and 430 nm. Therefore, the eight studied pesticides are susceptible to degradation upon exposure to the xenon lamp, which emits radiation between 280 and 550 nm. Meanwhile, five pesticides have absorption bands at wavelengths >295 nm: cyprodinil, pendimethalin, oxadiazon, fipronil, and difenoconazole. These five pesticides are potentially degradable upon solar exposure. The other three pesticides (deltamethrin, permethrin, and tetraconazole), have absorption bands below or around 295 nm, implying that these pesticides may or may not undergo photolysis via solar radiation.

3.2. Corrective factor F_{light}

To extrapolate the pesticide degradation results obtained from the xenon lamp in the laboratory to real atmosphere with solar irradiation, a corrective factor is calculated for each pesticide, to estimate its photolysis rate constant (J'). This factor corresponds to the ratio between the integrated area under the emission energy curve of the lamp and the integrated area under the average solar emission energy curve. The limits of these integrations are defined by the wavelength range specific to the absorption of the pesticide under study. The calculated corrective factors (F_{light}) are presented in Table 1.

Table 1
Corrective factors derived from integrating lamp and solar average emission spectra.

Pesticide	Absorption wavelength range (nm)	Integration area of the lamp's spectrum ($W{\cdot}m^{-2}$)	Integration area of the sun's spectrum ($W{\cdot}m^{-2}$)	F_{light}
Cyprodinil	280–359	26.29 ± 0.12	8.55 ± 0.06	3.07 ± 0.18
Oxadiazon	280–318	4.12 ± 0.04	0.90 ± 0.01	4.60 ± 0.05
Fipronil	280–319	4.42 ± 0.04	0.98 ± 0.01	4.53 ± 0.05
Difenoconazole	280–316	3.55 ± 0.04	0.75 ± 0.01	4.72 ± 0.05
Permethrin	280–299	0.72 ± 0.01	0.205 ± 0.01	3.53 ± 0.02
Deltamethrin	280–299	0.72 ± 0.01	0.21 ± 0.01	3.53 ± 0.02
Tetraconazole	280–298	0.64 ± 0.01	0.19 ± 0.01	3.36 ± 0.02
Pendimethalin	280–565	319.62 ± 0.46	185.93 ± 0.29	1.72 ± 0.80

The corrective factors listed in this table range from 1.72 for pendimethalin to 4.72 for difenoconazole.

3.3. Heterogeneous photolysis

The eight pesticides were separately adsorbed onto silica particles and exposed to a 300 W xenon lamp for 26 h. The decay of normalized

Table 2
First-order photolysis frequencies and atmospheric half-lives of the 8 pesticides exposed individually to the 300 W xenon lamp and their estimation under sun exposure.

Pesticide	Xenon lamp		Sun	
	J (s^{-1})	$t_{1/2}$ (days)[a]	J′ (s^{-1})	$t_{1/2}$ (days)[a]
Fipronil	$(1.7 \pm 0.1) \times 10^{-4}$	0.1	$(3.8 \pm 0.2) \times 10^{-5}$	0.4
Oxadiazon	$(3.4 \pm 0.1) \times 10^{-5}$	0.5	$(7.4 \pm 0.1) \times 10^{-6}$	2.2
Difenoconazole	$(1.4 \pm 0.1) \times 10^{-5}$	1.1	$(3.0 \pm 0.2) \times 10^{-6}$	5.3
Deltamethrin	$(1.1 \pm 0.1) \times 10^{-5}$	1.4	$(3.1 \pm 0.1) \times 10^{-6}$	5.2
Cyprodinil	$(9.2 \pm 0.3) \times 10^{-6}$	1.7	$(3.0 \pm 0.5) \times 10^{-6}$	5.3
Pendimethalin	$(5.9 \pm 0.4) \times 10^{-6}$	2.7	$(3.4 \pm 1.2) \times 10^{-6}$	4.7
Tetraconazole	$(1.2 \pm 0.3) \times 10^{-6}$	13.4	$(3.6 \pm 0.3) \times 10^{-7}$	44.6
Permethrin	$< (1.2 \pm 0.3) \times 10^{-6}$	>13.4	$< (3.4 \pm 0.3) \times 10^{-7}$	>47.2

[a] Atmospheric half-lives calculated for 12 h exposure per day.

concentrations relative to their initial concentration for the pesticides under study is shown in Fig. SI4. The photolysis rate constants and the atmospheric half-lives of the eight pesticides under study, when exposed to xenon lamp, as well as their estimated values under sunlight exposure, are presented in Table 2.

Results show that seven of the eight pesticides studied undergo significant direct photolytic degradation. The reactivity sequence is as follows: fipronil > oxadiazon > difenoconazole > deltamethrin > cyprodinil > pendimethalin > tetraconazole > permethrin. Despite being subjected to the same experimental conditions, the extent of degradation varies, ranging from low as 6 % for tebuconazole to over 98 % for both fipronil and oxadiazon after 26 h of exposure. Notably, only permethrin exhibits negligible degradation under these conditions.

The obtained photolysis frequencies vary $(1.7 \pm 0.1) \times 10^{-4}\ s^{-1}$ for fipronil to less than $(1.2 \pm 0.3) \times 10^{-6}\ s^{-1}$ for permethrin. Among the studied pesticides and under our irradiation conditions, fipronil exhibits the most rapid degradation rate. Its light-induced degradation rate is five times higher than that of oxadiazon and over 140 times higher than that of tetraconazole. Additionally, deltamethrin and permethrin, both pyrethroids, demonstrate distinct responses to light. Specifically, permethrin does not undergo photolysis under our experimental conditions, unlike deltamethrin, which has a half-life of 1.4 days. Indeed, our findings are consistent with existing literature studies on solid-phase, which have already shown that chlorinated pyrethroids like permethrin exhibit greater light stability compared to brominated pyrethroids such as deltamethrin (Fernández-Álvarez et al., 2007; Ruzo et al., 1982; Ruzo and Casida, 1980).

Additionally, the atmospheric half-lives presented range from 0.1 day for fipronil to over 13.4 days for permethrin (Table 2). However, these values cannot be directly extrapolated to real atmospheric conditions due to the difference in actinic flux between the xenon lamp and the sun. Nonetheless, it's crucial to note that atmospheric half-lives are inherently longer than those obtained in the reactor, given that the actinic flux from the lamp surpasses that of the sun.

The corrective factors presented in Table 1 for each pesticide enable the estimation of the photolysis rate constant (J′) and the atmospheric half-lives for 12 h of sunlight exposure per day (Table 2). In this context, J′ vary from $(3.8 \pm 0.2) \times 10^{-5}\ s^{-1}$ for fipronil to less than $(3.4 \pm 0.3) \times 10^{-7}\ s^{-1}$ for permethrin, indicating values lower than those determined using the xenon lamp.

The degradation rates under sunlight follow a different order compared to the previous sequence, and it is as follows: fipronil > oxadiazon > pendimethalin > deltamethrin > difenoconazole = cyprodinil > tetraconazole > permethrin. Additionally, atmospheric half-lives in this case range from 0.4 days for fipronil to over 47.2 days for permethrin.

3.4. Influence of pesticide mixture on photolysis degradation rates

We also investigated the stability of the photolysis rate constants for a pesticide when adsorbed individually on particles compared to a mixture of several pesticides. This aspect is crucial to verify that the kinetic constants determined in laboratory conditions with a specific mixture of pesticides remain valid for real atmospheric conditions where pesticides are associated on particles in highly diverse mixtures. To achieve this, an experiment was conducted under the same conditions as before, involving the simultaneous adsorption of eight pesticides on silica particles, followed by direct exposure to xenon lamp light for 8 h.

The temporal evolution of the eight pesticides in the mixture is shown in Fig. SI5, and the photolysis frequencies ($J_{mixture}$) obtained from these experiments are presented in Table 3.

Seven of the eight studied pesticides undergo degradation. The reactivity order for the pesticide mixture is as follows: fipronil > oxadiazon > cyprodinil > pendimethalin > deltamethrin > permethrin > tetraconazole. Only difenoconazole shows no significant loss after 8 h of exposure.

By comparing the results, a change in reactivity can be noted for certain pesticides. Fipronil, oxadiazon, difenoconazole, deltamethrin, and cyprodinil showed only slight modifications in reactivity, with a factor of change less than or equal to 3. This means that, within the uncertainty of the results, their behavior in the atmosphere will not be significantly altered. In contrast, pendimethalin, permethrin, and tetraconazole demonstrate an increase in their photo-degradation. The latter two pesticides degrade in the presence of the other seven adsorbed pesticides but show no or slower degradation when adsorbed alone.

This phenomenon can be explained by a photosensitization effect, where one pesticide absorbs xenon light and transfers this energy to another molecule, such as permethrin or tetraconazole (Gómez Alvarez et al., 2012). This is supported by the observation that permethrin and tetraconazole are not easily photolyzed when adsorbed alone. Additionally, for these two pesticides, there is little overlap between their absorption spectrum and the emission spectrum of the xenon lamp (cf. Fig. 2). Photosensitization thus enables them to absorb energy more efficiently, leading to their destabilization.

A previous study, (Dureja et al., 1984) demonstrated that the presence of a dinitroaniline-family pesticide with the 2,6-dinitroaniline group stabilized pyrethroids adsorbed on glass or silica gel against photodegradation. In our present study, pendimethalin, from the

Table 3
First-order photolysis frequencies and atmospheric half-lives of the 8 pesticides adsorbed separately or in combination, when exposed to 300 W xenon lamp.

Pesticide	$J_{separately}$ (s^{-1})	$t_{1/2}$ (days)[a]	$J_{mixture}$ (s^{-1})	$t_{1/2}$ (days)[a]
Fipronil	$(1.7 \pm 0.1) \times 10^{-4}$	0.1	$(5.1 \pm 0.3) \times 10^{-5}$	0.3
Oxadiazon	$(3.4 \pm 0.1) \times 10^{-5}$	0.5	$(2.6 \pm 0.2) \times 10^{-5}$	0.6
Difenoconazole	$(1.4 \pm 0.1) \times 10^{-5}$	1.1	$< (1.1 \pm 0.1) \times 10^{-5}$	>1.4
Deltamethrin	$(1.1 \pm 0.1) \times 10^{-5}$	1.4	$(1.9 \pm 0.3) \times 10^{-5}$	0.8
Cyprodinil	$(9.2 \pm 0.3) \times 10^{-6}$	1.7	$(2.1 \pm 0.2) \times 10^{-5}$	0.7
Pendimethalin	$(5.9 \pm 0.4) \times 10^{-6}$	2.7	$(1.9 \pm 0.2) \times 10^{-5}$	0.8
Tetraconazole	$(1.2 \pm 0.3) \times 10^{-6}$	13.4	$(1.1 \pm 0.1) \times 10^{-5}$	1.4
Permethrin	$< (1.2 \pm 0.3) \times 10^{-6}$	>13.4	$(1.5 \pm 0.2) \times 10^{-5}$	1.1

[a] Atmospheric half-lives calculated for 12 h exposure per day.

dinitroaniline family, does not stabilize the pyrethroids, deltamethrin and permethrin. Instead, it enhances the reactivity of permethrin and shows no significant modification in reactivity for deltamethrin.

The results obtained raise questions about the transferability of pesticide photolysis constants adsorbed on particulate phases obtained through laboratory experiments under controlled conditions to the real atmosphere, where pesticides coexist with an infinite mixture of other pesticides or semi-volatile organic compound (SVOCs) that may act as photosensitizers or photostabilizers.

This contrasts with our recent study (Samia et al., 2024), where no mixture effect was observed when investigating the heterogeneous atmospheric reactivity of pesticides towards ozone and OH radicals.

3.5. Comparison with pesticide's photolysis in the gas-phase

The available literature on the photolysis of pesticides in the gaseous phase does not cover the eight pesticides examined in this study. However, upon comparing the estimated sun exposure reactivity of pendimethalin from Table 2 with another pesticide from the same dinitroaniline family in Table 4, it becomes evident that photolysis in the particulate phase is significantly slower than in the gas phase since our pesticide exhibited a half-life of 4.7 days, while trifluralin, in four separate studies, presents a half-lives ranging from 20 min to 1 h.

Furthermore, when comparing the atmospheric half-lives of pesticides adsorbed on the particulate phase in this study (ranging from 10 h for fipronil to >47 days for permethrin) with those of pesticides in the gaseous phase reported in the literature (ranging from a couple of minutes for parathion to 8 h for chloropicrin) with methyl isothiocyanate, the only pesticide that exhibited an atmospheric half-life of two days in the gaseous phase, it is clear that pesticides are more reactive towards light in the gaseous phase than in the particulate phase.

These discrepancies were expected, as previous studies investigating pesticide reactivity with atmospheric oxidants in the particulate phase (Mattei et al., 2018, 2019a, 2019b, 2019c; Samia et al., 2024; Socorro et al., 2015, 2016a, 2016b) have demonstrated comparable behaviors. This could potentially be attributed to the presence of holes and crevices in the solid phase where pesticides might shield themselves from light radiations and atmospheric oxidants, leading to prolonged persistence in the solid phase and, consequently, in the atmosphere.

4. Atmospheric implications

By combining the photolysis half-lives obtained for the eight pesticides under study (considering estimations after exposure to sunlight and excluding the mixture effect) with their half-lives towards atmospheric oxidants (O_3, OH radicals, and NO_3 radicals) reported in the literature for the particulate phase, an overall half-life in this phase can be calculated using Eq. (6). The calculated half-lives are presented in Table 5.

Table 5
Overall half-lives of the eight pesticides under study in the particulate phase.

Pesticide	*hv* (days)[a]	O_3 (days)[b]	OH (days)[c]	NO_3 (days)[d]	Overall (days)
Fipronil	0.4	>24.0	>24.9	14.0	>0.4
Oxadiazon	2.2	>24.0	>24.9	10.9	>1.6
Difenoconazole	5.3	>24.0	>24.9	Unknown	>3.7
Deltamethrin	5.2	10.2	15.5	15.4	>2.4
Cyprodinil	5.3	9.2	11.0	11.2	2.1
Pendimethalin	4.7	24.0	24.9	16.1	2.8
Tetraconazole	44.6	>24.0	>24.9	7.6	>4.2
Permethrin	>47.2	13.6	19.4	8.6	>3.8

[a] This study.
[b] Atmospheric half-lives calculated for $[O_{3(gas)}] = 9{,}85 \times 10^{11}$ molecule·s·cm^{-3} with an exposure time of 24 h (Socorro et al., 2015).
[c] Atmospheric half-lives calculated for $[OH^{\bullet}_{(gas)}] = 1.5 \times 10^{6}$ molecules·cm^{-3} with an exposure time of 12 h (Socorro et al., 2016a).
[d] Atmospheric half-lives calculated for $[NO_{3(gas)}] = 5 \times 10^{8}$ molecules·cm^{-3} with an exposure of 12 h (Mattei et al., 2019c).

$$\frac{1}{t_{1/2\ Overall\ (part)}} = \frac{1}{t_{1/2\ hv_{(part)}}} + \frac{1}{t_{1/2_{O_3\ (part)}}} + \frac{1}{t_{1/2_{OH_{(part)}}}} + \frac{1}{t_{1/2\ NO_3\ (part)}} \quad (6)$$

The overall half-lives range from 0.4 days for fipronil to >4.2 days for tetraconazole. It is notable that the prevailing degradation pathway for these pesticides is direct photolysis, followed by NO_3 radicals oxidation for tetraconazole and permethrin in the particulate phase. In fact, according to the guidelines of the Stockholm Convention (2001), an organic compound with atmospheric half-life of 2 days or more is classified as a Persistent Organic Pollutant (POP). Considering the half-lives presented above, six of these eight pesticides can be classified as POPs. The two exceptions are fipronil and oxadiazon.

However, this conclusion is not entirely accurate, as the half-life values do not account the partitioning of these pesticides between the gaseous and particulate phases, which is crucial to accurately simulating atmospheric processes.

5. Conclusion

This study provides a first estimation of the photolysis rates of eight pesticides (Cyprodinil, deltamethrin, difenoconazole, fipronil, oxadiazon, pendimethalin, permethrin, and tetraconazole) adsorbed on silica particles and exposed to a 300 W xenon lamp and 55 % RH. Under these experimental conditions, fipronil exhibited the highest reactivity with a photolysis rate of $(1.7 \pm 0.1) \times 10^{-4}$ s^{-1}, whereas tetraconazole and permethrin showed very slow degradation rates $\leq (1.2 \pm 0.3) \times 10^{-6}$ s^{-1}. Photolysis rates for the other pesticides ranged from $(5.9 \pm 0.3) \times 10^{-6}$ to $(3.4 \pm 0.1) \times 10^{-5}$ s^{-1}, with pendimethalin being the slowest, followed by cyprodinil, deltamethrin, difenoconazole, and oxadiazon.

When extrapolated to actual sunlight conditions, the calculated

Table 4
Photolysis frequencies available in the literature for pesticides in the gaseous phase (studied separately) and corresponding atmospheric half-lives.

Chemical family	Pesticide	Temperature (°C)	RH (%)	Light source	$J_{photolysis\ (gas)}$ (s^{-1})	$t_{1/2}$ (hours)[a]	References
Dinitroaniline	Trifluralin	Unknown	Unknown	Sunlight	$(3.8 \pm 2.3) \times 10^{-4}$	1.0	Mongar and Miller (1988)
		29 ± 1	20–30	Sunlight	$\sim 5.7 \times 10^{-4}$	~0.7	Woodrow et al. (1978)
		60–80	Unknown	Xenon	$(5.0 \pm 0.2) \times 10^{-4}$[b]	0.8	Hebert et al. (2000)
		<32	Unknown	Sunlight	$(1.2 \pm 0.5) \times 10^{-3}$	0.3	Le Person et al. (2007)
	Ethafluralin	27 ± 5	Unknown	Sunlight	$(1.3 \pm 0.2) \times 10^{-3}$	0.3	Muñoz et al. (2014)
Organophosphorus	Phorate	Unknown	Unknown	Sunlight	$(2.2 \pm 0.7) \times 10^{-3}$	0.2	Hebert et al. (1998)
	Parathion	29 ± 1	20–30	Sunlight	$\sim 5.7 \times 10^{-3}$	0.1	Woodrow et al. (1978)
	Chlorpyrifos	60–80	Unknown	Xenon	1.9×10^{-4}–9.6×10^{-5}[b]	2.0–4.0	Hebert et al. (2000)
Organochlorine	Chloropicrin	Unknown	Unknown	Sunlight	$\sim 5.7 \times 10^{-5}$	6.7	Carter et al. (1997)
		25 ± 5	<2	Sunlight	$\sim 5.1 \times 10^{-5}$	7.5	Vera et al. (2010)
Carbamate	Methyl Isothiocyanate	26 ± 16	Unknown	Sunlight	$\sim 6.7 \times 10^{-6}$	57.5	Geddes et al. (1995)

[a] Atmospheric half-lives calculated for 12 h exposure per day.
[b] Values corrected for sunlight exposure.

photolysis frequencies and atmospheric half-life values, reveal significant variations in photolysis constants. Furthermore, the study evaluated the impact of pesticide mixtures on the photolysis rate constant of each pesticide revealing noticeable influences. Specifically, in the presence of a pesticide cocktail, permethrin and tetraconazole exhibited increased reactivity, while others showed no significant change. This underscores the complex interactions between pesticides on aerosol surfaces.

These works highlight the importance of considering pesticide photolysis in the particulate phase when assessing their fate in the atmosphere as it represents a significant degradation pathway for pesticides.

For future studies, it would be interesting to calculate the quantum yields of the pesticides under study, for more precise values of their atmospheric persistence. Additionally, using a solar simulator or conducting experiments directly in an outdoor atmospheric simulation chamber would enhance understanding of direct pesticide photolysis under clear conditions.

CRediT authorship contribution statement

Boulos Samia: Writing – original draft, Investigation, Data curation. **Joanna Socorro:** Methodology, Investigation, Data curation. **Amandine Durand:** Writing – review & editing, Methodology, Investigation. **Etienne Quivet:** Validation, Supervision, Funding acquisition. **Henri Wortham:** Writing – review & editing, Validation, Supervision, Conceptualization.

Declaration of competing interest

The authors declare that they have no known competing financial interests or personal relationships that could have appeared to influence the work reported in this paper.

Data availability

Data will be made available on request.

Acknowledgment

This work was supported by the A*MIDEX project (no. ANR-11-IDEX-0001-02) funded by the “Investissements d'Avenir” French Government Program, managed by the French National Research Agency (ANR).

Appendix A. Supplementary data

Supplementary data to this article can be found online at https://doi.org/10.1016/j.scitotenv.2024.174964.

References

Abbott, I.M., Bonsall, J.L., Chester, G., Hart, T.B., Turnbull, G.J., 1987. Worker exposure to a herbicide applied with ground sprayers in the United Kingdom. Am. Ind. Hyg. Assoc. J. 48, 167–175. https://doi.org/10.1080/15298668791384571.

Aregahegn, K.Z., Ezell, M.J., Finlayson-Pitts, B.J., 2018. Photochemistry of solid films of the neonicotinoid nitenpyram. Environ. Sci. Technol. 52, 2760–2767. https://doi.org/10.1021/acs.est.7b06011.

Aschmann, S.M., Atkinson, R., 2006. Kinetic and product study of the gas-phase reactions of OH radicals, NO3 radicals, and O3 with (C2H5O)2P(S)CH3 and (C2H5O)3PS. J. Phys. Chem. A 110, 13029–13035. https://doi.org/10.1021/jp065382v.

Aschmann, S.M., Tuazon, E.C., Atkinson, R., 2005a. Atmospheric chemistry of diethyl methylphosphonate, diethyl ethylphosphonate, and triethyl phosphate. J. Phys. Chem. A 109, 2282–2291. https://doi.org/10.1021/jp0446938.

Aschmann, S.M., Tuazon, E.C., Atkinson, R., 2005b. Atmospheric chemistry of dimethyl phosphonate, dimethyl methylphosphonate, and dimethyl ethylphosphonate. J. Phys. Chem. A 109, 11828–11836. https://doi.org/10.1021/jp055286e.

Borrás, E., Ródenas, M., Vera, T., Gómez, T., Muñoz, A., 2017. Atmospheric degradation of the organothiophosphate insecticide – Pirimiphos-methyl. Sci. Total Environ. 579, 1–9. https://doi.org/10.1016/j.scitotenv.2016.11.009.

Bossan, D., Wortham, H., Masclet, P., 1995. Atmospheric transport of pesticides adsorbed on aerosols I. Photodegradation in simulated atmosphere. Chemosphere 30, 21–29. https://doi.org/10.1016/0045-6535(94)00372-2.

Carter, W.P.L., Luo, D., Malkina, I.L., 1997. Investigation of the atmospheric reactions of chloropicrin. Atmos. Environ. 31, 1425–1439. https://doi.org/10.1016/S1352-2310(96)00324-X.

Cheng, S., Sun, S., Zhang, H., 2017. Theoretical study on the reaction mechanism of carbaryl with NO3 radical. Theor. Chem. Accounts 136, 60. https://doi.org/10.1007/s00214-017-2093-z.

Désert, M., Ravier, S., Gille, G., Quinapallo, A., Armengaud, A., Pochet, G., Savelli, J.-L., Wortham, H., Quivet, E., 2018. Spatial and temporal distribution of current-use pesticides in ambient air of Provence-Alpes-Côte-d'Azur Region and Corsica, France. Atmos. Environ. 192, 241–256. https://doi.org/10.1016/j.atmosenv.2018.08.054.

Dureja, P., Casida, J.E., Ruzo, L.O., 1984. Dinitroanilines as photostabilizers for pyrethroids. J. Agric. Food Chem. 32, 246–250. https://doi.org/10.1021/jf00122a017.

Fernández-Álvarez, M., Sánchez-Prado, L., Lores, M., Llompart, M., García-Jares, C., Cela, R., 2007. Alternative sample preparation method for photochemical studies based on solid phase microextraction: synthetic pyrethroid photochemistry. J. Chromatogr. A 1152, 156–167. https://doi.org/10.1016/j.chroma.2006.12.095. Advances in Sample Preparation.

Figueiredo, A., Strekowski, R.S., Bosland, L., Durand, A., Wortham, H., 2020. Photolytic degradation of molecular iodine adsorbed on model SiO2 particles. Sci. Total Environ. 723, 137951 https://doi.org/10.1016/j.scitotenv.2020.137951.

Finlayson-Pitts, B., Pitts, J., 2000. Chemistry of Upper and Lower Atmosphere. https://doi.org/10.1016/B978-012257060-5/50010-1.

Geddes, J.D., Miller, G.C., Taylor, G.E., 1995. Gas phase photolysis of methyl isothiocyanate. Environ. Sci. Technol. 29, 2590–2594. https://doi.org/10.1021/es00010a020.

Glotfelty, D.E., Leech, M.M., Jersey, J., Taylor, A.W., 1989. Volatilization and wind erosion of soil surface applied atrazine, simazine, alachlor, and toxaphene. J. Agric. Food Chem. 37, 546–551. https://doi.org/10.1021/jf00086a059.

Gómez Alvarez, E., Wortham, H., Strekowski, R., Zetzsch, C., Gligorovski, S., 2012. Atmospheric photosensitized heterogeneous and multiphase reactions: from outdoors to indoors. Environ. Sci. Technol. 46, 1955–1963. https://doi.org/10.1021/es2019675.

Gueymard, C.A., Myers, D., Emery, K., 2002. Proposed reference irradiance spectra for solar energy systems testing. Sol. Energy 73, 443–467. https://doi.org/10.1016/S0038-092X(03)00005-7.

Gupte, S., Mohandas, P.I.T., Conrad, J.M., 2012. A survey of quadrotor unmanned aerial vehicles. In: 2012 Proc. IEEE Southeastcon, pp. 1–6.

HEAL, 2023. Health and Environment Alliance | Infographic: The Impact of Harmful Pesticides on people's Health and the Environment. Health Environ. Alliance. URL. https://www.env-health.org/infographic-the-impact-of-harmful-pesticides-on-peoples-health-and-the-environment/ (accessed 1.14.24).

Hebert, V.R., Geddes, J.D., Mendosa, J., Miller, G.C., 1998. Gas-phase photolysis of phorate, a phosphorothioate insecticide. Chemosphere 36, 2057–2066. https://doi.org/10.1016/S0045-6535(97)10090-X.

Hebert, V.R., Hoonhout, C., Miller, G.C., 2000. Use of stable tracer studies to evaluate pesticide photolysis at elevated temperatures. J. Agric. Food Chem. 48, 1916–1921. https://doi.org/10.1021/jf990699w.

Le Person, A., Mellouki, A., Muñoz, A., Borras, E., Martin-Reviejo, M., Wirtz, K., 2007. Trifluralin: photolysis under sunlight conditions and reaction with HO radicals. Chemosphere 67, 376–383. https://doi.org/10.1016/j.chemosphere.2006.09.023.

Li, S., Nianogo, R.A., Lin, Y., Wang, H., Yu, Y., Paul, K.C., Ritz, B., 2024. Cost-effectiveness analysis of insecticide ban aimed at preventing Parkinson's disease in Central California. Sci. Total Environ. 912, 168913 https://doi.org/10.1016/j.scitotenv.2023.168913.

Mattei, C., Wortham, H., Quivet, E., 2018. Heterogeneous atmospheric degradation of pesticides by ozone: influence of relative humidity and particle type. Sci. Total Environ. 625, 1544–1553. https://doi.org/10.1016/j.scitotenv.2018.01.049.

Mattei, C., Dupont, J., Wortham, H., Quivet, E., 2019a. Influence of pesticide concentration on their heterogeneous atmospheric degradation by ozone. Chemosphere 228, 75–82. https://doi.org/10.1016/j.chemosphere.2019.04.082.

Mattei, C., Wortham, H., Quivet, E., 2019b. Heterogeneous atmospheric degradation of current-use pesticides by nitrate radicals. Atmos. Environ. 211, 170–180. https://doi.org/10.1016/j.atmosenv.2019.05.016.

Mattei, C., Wortham, H., Quivet, E., 2019c. Heterogeneous degradation of pesticides by OH radicals in the atmosphere: influence of humidity and particle type on the kinetics. Sci. Total Environ. 664, 1084–1094. https://doi.org/10.1016/j.scitotenv.2019.02.038.

Meylan, W.M., Howard, P.H., 1993. Computer estimation of the atmospheric gas-phase reaction rate of organic compounds with hydroxyl radicals and ozone. Chemosphere 26, 2293–2299. https://doi.org/10.1016/0045-6535(93)90355-9.

Mongar, K., Miller, G.C., 1988. Vapor phase photolysis of trifluralin in an outdoor chamber. Chemosphere 17, 2183–2188. https://doi.org/10.1016/0045-6535(88)90166-X.

Muñoz, A., Vera, T., Ródenas, M., Borrás, E., Mellouki, A., Treacy, J., Sidebottom, H., 2014. Gas-phase degradation of the herbicide ethalfluralin under atmospheric conditions. Chemosphere 95, 395–401. https://doi.org/10.1016/j.chemosphere.2013.09.053.

Natu, A.S., Kulkarni, S.C., 2016. Adoption and utilization of drones for advanced precision farming: a review. Int. J. Recent Innov. Trends Comput. Commun. 4, 563–565.

Pardo, L.A., Beane Freeman, L.E., Lerro, C.C., Andreotti, G., Hofmann, J.N., Parks, C.G., Sandler, D.P., Lubin, J.H., Blair, A., Koutros, S., 2020. Pesticide exposure and risk of

aggressive prostate cancer among private pesticide applicators. Environ. Health 19, 30. https://doi.org/10.1186/s12940-020-00583-0.

Paul, K.C., Krolewski, R.C., Moreno, E.L., Blank, J., Holton, K., Ahfeldt, T., Furlong, M., Yu, Y., Cockburn, M., Thompson, L.K., Bronstein, J., Rubin, L.L., Khurana, V., Ritz, B., 2022. Coupling Comprehensive Pesticide-wide Association Study to iPSC Dopaminergic Screening Identifies and Classifies Parkinson-relevant Pesticides. https://doi.org/10.1101/2022.02.06.479305.

Pimentel, D., Levitan, L., 1986. Pesticides: amounts applied and amounts reaching pests. BioScience 36, 86–91. https://doi.org/10.2307/1310108.

Pisa, L., Goulson, D., Yang, E.-C., Gibbons, D., Sánchez-Bayo, F., Mitchell, E., Aebi, A., van der Sluijs, J., MacQuarrie, C.J.K., Giorio, C., Long, E.Y., McField, M., Bijleveld van Lexmond, M., Bonmatin, J.-M., 2021. An update of the Worldwide Integrated Assessment (WIA) on systemic insecticides. Part 2: impacts on organisms and ecosystems. Environ. Sci. Pollut. Res. 28, 11749–11797. https://doi.org/10.1007/s11356-017-0341-3.

Ruzo, L.O., Casida, J.E., 1980. Pyrethroid photochemistry: mechanistic aspects in reactions of the (dihalogenovinyl)cyclopropanecarboxylate substituent. J. Chem. Soc. Perkin 1, 728–732. https://doi.org/10.1039/P19800000728.

Ruzo, L.O., Smith, I.H., Casida, J.E., 1982. Pyrethroid photochemistry: photooxidation reactions of the chrysanthemates phenothrin and tetramethrin. J. Agric. Food Chem. 30, 110–115. https://doi.org/10.1021/jf00109a025.

Samia, B., Della Puppa, L., Mattei, C., Durand, A., Ravier, S., Quivet, E., Wortham, H., 2024. Influence of pesticide mixture on their heterogeneous atmospheric degradation by ozone and OH radicals. Environ. Pollut., 123351 https://doi.org/10.1016/j.envpol.2024.123351.

Sauret, N., Wortham, H., Putaud, J.-P., Mirabel, P., 2008. Study of the effects of environmental parameters on the gas/particle partitioning of current-use pesticides in urban air. Atmos. Environ. 42, 544–553. https://doi.org/10.1016/j.atmosenv.2007.09.012.

Seinfeld, J.H., Pandis, S.N., 2016. Atmospheric Chemistry and Physics: From Air Pollution to Climate Change. John Wiley & Sons.

Socorro, J., Gligorovski, S., Wortham, H., Quivet, E., 2015. Heterogeneous reactions of ozone with commonly used pesticides adsorbed on silica particles. Atmos. Environ. 100, 66–73. https://doi.org/10.1016/j.atmosenv.2014.10.044.

Socorro, J., Durand, A., Temime-Roussel, B., Gligorovski, S., Wortham, H., Quivet, E., 2016a. The persistence of pesticides in atmospheric particulate phase: an emerging air quality issue. Sci. Rep. 6, 33456. https://doi.org/10.1038/srep33456.

Socorro, J., Marque, S.R.A., Temime-Roussel, B., Ravier, S., Gligorovski, S., Wortham, H., Quivet, E., 2016b. Products and mechanisms of the heterogeneous reactions of ozone with commonly used pyrethroids in the atmosphere. Sci. Total Environ. 573, 1287–1293. https://doi.org/10.1016/j.scitotenv.2016.06.217.

Vera, T., Munoz, A., Ródenas, M., Vázquez, M., Mellouki, A., Treacy, J., Mulla, I.A., Sidebottom, H., 2010. Photolysis of trichloronitromethane (chloropicrin) under atmospheric conditions. Z. Für Phys. Chem. 224, 1039–1057. https://doi.org/10.1524/zpch. 2010.6140.

Vera, T., Borrás, E., Chen, J., Coscollá, C., Daële, V., Mellouki, A., Ródenas, M., Sidebottom, H., Sun, X., Yusá, V., Zhang, X., Muñoz, A., 2015. Atmospheric degradation of lindane and 1,3-dichloroacetone in the gas phase. Studies at the EUPHORE simulation chamber. Chemosphere 138, 112–119. https://doi.org/10.1016/j. chemosphere.2015.05.061.

Woodrow, J.E., Crosby, D.G., Mast, T., Moilanen, K.W., Seiber, J.N., 1978. Rates of transformation of trifluralin and parathion vapors in air. J. Agric. Food Chem. 26, 1312–1316. https://doi.org/10.1021/jf60220a019.

Ye, M., Beach, J., Martin, J.W., Senthilselvan, A., 2017. Pesticide exposures and respiratory health in general populations. J. Environ. Sci. 51, 361–370. https://doi.org/10.1016/j.jes.2016. 11.012.

Zhou, Q., Sun, X., Gao, R., Zhang, Q., Wang, W., 2010. Mechanism study on OH-initiated atmospheric degradation of the organophosphorus pesticide chlorpyrifos. J. Mol. Struct. THEOCHEM 952, 8–15. https://doi.org/10.1016/j.theochem.2010.03.023.

Zhou, Q., Sun, X., Gao, R., Hu, J., 2011. Mechanism and kinetic properties for OH-initiated atmospheric degradation of the organophosphorus pesticide diazinon. Atmos. Environ. 45, 3141–3148. https://doi.org/10.1016/j.atmosenv.2011.02.064.

Zivan, O., Segal-Rosenheimer, M., Dubowski, Y., 2016. Airborne organophosphate pesticides drift in Mediterranean climate: the importance of secondary drift. Atmos. Environ. 127, 155–162. https://doi.org/10.1016/j.atmosenv.2015.12.003.